

EXPANSION OF A CYLINDRICAL CAVITY IN SAND

VOLODIA A. OSINOV AND ROBERTO CUDMANI

*Institute of Soil Mechanics and Rock Mechanics,
University of Karlsruhe, 76128 Karlsruhe, Germany
osinov@ibf-tiger.bau-verm.uni-karlsruhe.de
cudmani@ibf-tiger.bau-verm.uni-karlsruhe.de*

(Received 20 April 2000)

Abstract: The paper presents numerical solution to the problem of the symmetric quasi-static large-strain expansion of a cylindrical cavity in sand. The boundary value problem is solved with the use of a constitutive equation of hypoplasticity calibrated for a particular sand. As the radius of the cavity increases, the stresses and the density on the cavity surface asymptotically approach limit values which correspond to a so-called critical state of the sand. The limit values depend on the initial stresses and the initial density. The solutions are compared with experimental results for the same sand available in the literature. A comparison is also made with numerical solutions obtained by other authors.

Keywords: cavity expansion, sand, hypoplasticity, critical state

1. Introduction

The problem of expansion of a cavity in a plastic body has various applications and has been extensively studied. The present paper deals with the expansion of a cylindrical cavity in granular soil. Cylindrical and spherical cavities in soil were studied with the use of various elasto-plastic models by Vesić [1], Carter *et al.* [2], Yu and Houlsby [3], Collins *et al.* [4], Shuttle and Jefferies [5] and others.

Investigations of the cylindrical or spherical cavity expansion problem for soils are in most cases aimed at finding the limit state which the soil at the cavity wall asymptotically approaches as the radius of the cavity increases. This problem involves both geometrical and physical nonlinearities. The limit state at the cavity wall is attained when the radius of the cavity becomes at least two-three times as large as the initial radius, depending on the density. It is therefore necessary to take into account the geometrical nonlinearity caused by the large deformations. Note that in certain cases, when using relatively simple elasto-plastic constitutive

equations, it may be possible to obtain a semi-analytical solution for the expansion from zero to a finite radius and thus to find the limit state (Collins *et al.* [4]). Another difficulty consists in the fact that a soil is a physically nonlinear medium whose response essentially depends on the current stresses and density. Therefore, the constitutive equation used in the modelling must adequately describe the behaviour of the soil in the whole range of stresses and density covered during the cavity expansion.

The present paper presents a large-strain analysis of the symmetric quasi-static expansion of a cylindrical cavity in a cohesionless granular soil. The constitutive behaviour of the soil is described by a constitutive equation of hypoplasticity calibrated for a particular soil (Ticino sand). The expansion of a cavity is governed by a system of first-order partial differential equations. The boundary value problem is solved numerically by a finite-difference technique. The solutions are compared with experimental results on pressuremeter tests available in the literature. A comparison is also made with numerical solutions for the same sand obtained by other authors with the use of a different constitutive model.

2. Constitutive equation

The mechanical behaviour of granular soils at strains over 10^{-5} – 10^{-4} is physically nonlinear and requires the use of a proper plasticity model. In many cases, where the deformation does not involve multi-cycle loading, it may be assumed that the state of a dry cohesionless soil is fully determined by the current Cauchy stress tensor \mathbf{T} and the density, the latter being expressed in terms of the void ratio $e = (V - V_s) / V_s$, where V_s is the volume of the solid fraction and V is the total volume. This assumption forms the basis for the hypoplasticity theory [6–9]. A hypoplastic constitutive equation establishes a relationship between the stress rate $\dot{\mathbf{T}}$ (the material time derivative or, in general, an objective stress rate) and the rate of deformation \mathbf{D} (the symmetric part of the velocity gradient):

$$\dot{\mathbf{T}} = \mathbf{H}(\mathbf{T}, \mathbf{D}, e). \quad (1)$$

The tensor-valued function \mathbf{H} in (1) involves the current stress tensor and the void ratio and is nonlinear in all the arguments. As distinct from elastic-plastic models, hypoplasticity describes the plastic behaviour of a material with the help of a single equation without resolution of the deformation into elastic and plastic parts and without introducing the notions of loading, unloading and yield surface.

The hypoplastic constitutive equation in the version of Wolfersdorff [8] is written as:

$$\dot{\mathbf{T}} = f_b f_e \frac{1}{\text{tr}(\hat{\mathbf{T}}^2)} \left[F^2 \mathbf{D} + a^2 \text{tr}(\hat{\mathbf{T}}\mathbf{D})\hat{\mathbf{T}} + f_d a F(\hat{\mathbf{T}} + \hat{\mathbf{T}}^*) \|\mathbf{D}\| \right], \quad (2)$$

where

$$\hat{\mathbf{T}} = \frac{\mathbf{T}}{\text{tr} \mathbf{T}}, \quad \hat{\mathbf{T}}^* = \hat{\mathbf{T}} - \frac{1}{3} \mathbf{I}, \quad \|\mathbf{D}\| = \sqrt{\text{tr}(\mathbf{D}\mathbf{D})}, \quad (3)$$

and \mathbf{I} is the unit tensor. Function (2) is a modification of the relation given by Gudehus [6] and Bauer [7].

The coefficients in (2) depend on the invariants of the stress tensor and on the void ratio, which signifies the dependence of the stiffness on the current stresses and density. Since the function (2) is homogeneous of degree one in \mathbf{D} , the behaviour of the material is rate-independent. The term $\|\mathbf{D}\|$ does not allow the constitutive function to be linearized in the vicinity of $\mathbf{D} = \mathbf{0}$ and to be written in an incrementally linear form. A detailed representation of the coefficients involved in (2) and the constitutive parameters of Ticino sand are given in the Appendix.

The constitutive equation (1) is an evolution equation for the stress tensor $\mathbf{T}(t)$ with the time-dependent parameter $\mathbf{D}(t)$. The void ratio $e(t)$ is the other time-dependent parameter determined from the evolution equation:

$$\dot{e} = (1 + e) \text{tr} \mathbf{D}, \quad (4)$$

which expresses the balance of mass. If the “direction” of deformation $\mathbf{D} / \|\mathbf{D}\|$ is kept constant and there is no volume change ($\text{tr} \mathbf{D} = 0$), the function $\mathbf{T}(t)$ asymptotically approaches a certain value (a stationary point of the evolution equation (1)) which depends on the initial stress, density and the direction of deformation. In terms of soil mechanics, such stationary point is a so-called critical state [10–12] defined by the conditions:

$$\dot{\mathbf{T}} = \mathbf{0}, \quad \text{tr} \mathbf{D} = 0, \quad (\mathbf{D} \neq \mathbf{0}). \quad (5)$$

The void ratio e_c in a critical state and the corresponding pressure $p = -\text{tr} \mathbf{T} / 3$ ($\text{tr} \mathbf{T} < 0$ for compression) are assumed to be connected by the relation:

$$e_c = e_{c0} \exp \left[- \left(\frac{3p}{h_s} \right)^n \right], \quad (6)$$

where e_{c0} , h_s , n are material constants (see the Appendix). The critical void ratio at zero pressure e_{c0} is taken equal to the quantity e_{max} which corresponds to the looses state and is conventionally used in soil mechanics. The same pressure dependence is postulated for the minimal possible void ratio e_d at a given pressure p :

$$e_d = e_{d0} \exp \left[- \left(\frac{3p}{h_s} \right)^n \right]. \quad (7)$$

The material constant e_{d0} is the minimal void ratio at zero pressure that is taken equal to the void ratio e_{min} in the densest state obtained in the laboratory by the use of a standard technique. The relative density (also called the density index):

$$I_D = \frac{e_{max} - e}{e_{max} - e_{min}}, \quad (8)$$

usually used as a characteristic of density of a granular soil, does not imply pressure dependence of e_{min} and e_{max} . With (6) and (7) we can modify this quantity and introduce the pressure-dependent relative density:

$$I_D^* = \frac{e_c - e}{e_c - e_d}. \quad (9)$$

As an alternative to void ratio, this quantity will be used below as a characteristic of density of the material in the initial state at nonzero pressure prior to the expansion of the cavity. The modified relative density I_D^* is negative if the void ratio is higher than the critical void ratio for a given pressure.

3. Boundary value problem

Consider an infinitely long cylindrical cavity which expands quasi-statically and symmetrically, starting from an initial radius r_a^0 . The domain where the solution is sought is bounded by an outer cylindrical surface concentric with the cavity. In the cylindrical coordinates r, θ, z , the symmetric expansion of a cavity under the plane strain conditions is described by the velocity component v_r , the stress components $T_{rr}, T_{\theta\theta}, T_{zz}$ and the void ratio e . All these quantities are functions of radius r and time t . The stretching tensor has two nonzero components $D_{rr} = \partial v_r / \partial r$ and $D_{\theta\theta} = v_r / r$. For brevity, we will write $T_r, T_\theta, T_z, v, D_r, D_\theta$ instead of $T_{rr}, T_{\theta\theta}, T_{zz}, v_r, D_{rr}, D_{\theta\theta}$.

Under the assumed symmetry, the process of deformation is governed by a system of five first-order partial differential equations for the unknown functions v, T_r, T_θ, T_z and e . The system consists of the equilibrium equation:

$$\frac{\partial T_r}{\partial r} + \frac{1}{r}(T_r - T_\theta) = 0, \quad (10)$$

the constitutive equations (1):

$$\frac{\partial T_r}{\partial t} + v \frac{\partial T_r}{\partial r} = H_r \left(T_r, T_\theta, T_z, \frac{\partial v}{\partial r}, \frac{v}{r}, e \right), \quad (11)$$

$$\frac{\partial T_\theta}{\partial t} + v \frac{\partial T_\theta}{\partial r} = H_\theta \left(T_r, T_\theta, T_z, \frac{\partial v}{\partial r}, \frac{v}{r}, e \right), \quad (12)$$

$$\frac{\partial T_z}{\partial t} + v \frac{\partial T_z}{\partial r} = H_z \left(T_r, T_\theta, T_z, \frac{\partial v}{\partial r}, \frac{v}{r}, e \right), \quad (13)$$

and the mass balance equation (4):

$$\frac{\partial e}{\partial t} + v \frac{\partial e}{\partial r} = (1+e) \left(\frac{\partial v}{\partial r} + \frac{v}{r} \right). \quad (14)$$

Let $r_a(t)$ and $r_b(t)$ be the radii of the inner and the outer cylindrical surfaces, respectively, which bound the domain where the solution is sought. The initial radii are denoted by r_a^0 and r_b^0 . The case $r_b^0 = \infty$ corresponds to a cavity in an infinite body.

The boundary value problem for the system (10)–(14) is formulated as follows: given initial conditions

$$T_r^0(r), T_\theta^0(r), T_z^0(r), e^0(r) \quad (15)$$

at $t=0$, find the solution $v(r, t)$, $T_r(r, t)$, $T_\theta(r, t)$, $T_z(r, t)$, $e(r, t)$ for $t \geq 0$ with a given velocity at the inner boundary and a constant radial stress at the outer boundary, that is, with the boundary conditions:

$$\dot{r}_a(t) = v_0 > 0 \quad \text{and} \quad \dot{T}_r(r_b, t) = 0. \quad (16)$$

The initial stresses in (15) must satisfy the equilibrium equation (10). In the calculations presented below the initial stresses and density are taken to be homogeneous: $T_r^0 = T_\theta^0$, $T_z^0 = T_r^0 / K$ with a coefficient K . In this case, as follows from the equations, the solution to the problem with $r_b^0 = \infty$ and any r_a^0 can be obtained from the solution with $r_a^0 = 1$ merely by rescaling the r -axis. Since the behaviour of the material is rate-independent, the variable t plays the role of a loading parameter rather than physical time. For this reason, the value of v_0 in (16) can be chosen arbitrarily. The second condition in (16) may be replaced with $v(r_b, t) = 0$, which gives the same result if $r_b = \infty$. However, in most calculations we used the condition of constant pressure because this was found to give a better approximation to an infinite body if r_b is large but finite.

4. Numerical algorithm

The differentiation of the equilibrium equation (10) with respect to time and the use of the constitutive relations (11), (12) leads to the equation:

$$\frac{\partial H_r}{\partial r} + \frac{1}{r}(H_r - H_\theta) + \frac{\partial T_r}{\partial r} \left(\frac{v}{r} - \frac{\partial v}{\partial r} \right) = 0. \quad (17)$$

This is a second-order ordinary differential equation for the velocity $v(r, t)$ as functions of r at a fixed t . The integration of this equation requires two boundary conditions expressed in terms of velocity and/or its gradient $\partial v / \partial r$. Namely, one needs either one boundary condition at each point r_a and r_b to solve the two-point boundary value problem, or two boundary conditions (velocity and its gradient) at one point to solve the Cauchy problem.

The solution of the whole problem involves two integration procedures: 1) the integration of (17) from r_a to r_b with the boundary conditions (16) to find the velocity at a fixed time; and 2) the integration of (11)–(14) with respect to time to find the functions $T_r(r, t)$, $T_\theta(r, t)$, $T_z(r, t)$ and $e(r, t)$. The integration of (11)–(14) does not require any boundary conditions.

To integrate (17), the interval $[r_a, r_b]$ is divided into subintervals by introducing discretization points $r_{(j)}$, $j = 0, \dots, N$, where $r_{(0)} = r_a$, $r_{(N)} = r_b$. These points are treated as material points so that their coordinates $r_{(j)}$ are changed with the deformation. Rather than use boundary conditions at r_a and r_b immediately as dictated by (16), we prescribe two boundary conditions at r_a , namely velocity and its gradient $g = \partial v / \partial r$. To satisfy the boundary condition at r_b , the value of g at r_a is varied in order to find the right one. With the use of the Newton method which is commonly used for the solution of nonlinear equations, only a few iterations are needed. The boundary value problem is thus reduced to a sequence of the Cauchy problems. The advantage of this approach is the following. To solve the boundary value problem immediately, it would be necessary to solve a nonlinear system of N equations in N variables $v_{(1)}, \dots, v_{(N)}$. To solve the Cauchy problem, we start from the point $r_{(0)} = r_a$ and proceed to the points $r_{(1)}, r_{(2)}, \dots$ so that at each step we have to solve only one nonlinear equation in one variable (formula (19) below).

Equation (17) can be viewed as that of the first order with respect to H_r . In order to obtain the velocity $v_{(j+1)}$ from given $v_{(j)}$ and $g_{(j)}$ and thus to perform the step-by-step integration with respect to r , an implicit Euler scheme is applied to the function H_r :

$$H_{r_{(j+1)}} = H_{r_{(j)}} + \frac{1}{2} \left\{ \left. \frac{\partial H_r}{\partial r} \right|_{(j)} + \left. \frac{\partial H_r}{\partial r} \right|_{(j+1)} \right\} \Delta r_{(j)}, \quad (18)$$

where $\Delta r_{(j)} = r_{(j+1)} - r_{(j)}$. The use of (17) gives:

$$H_{r_{(j+1)}} - \frac{1}{2} \Omega_{(j+1)} \Delta r_{(j)} = H_{r_{(j)}} + \frac{1}{2} \Omega_{(j)} \Delta r_{(j)}, \quad (19)$$

where we have denoted:

$$\Omega = \frac{1}{r} (H_\theta - H_r) + \frac{\partial T_r}{\partial r} \left(g - \frac{v}{r} \right). \quad (20)$$

After substituting:

$$v_{(j+1)} = v_{(j)} + \frac{1}{2} (g_{(j)} + g_{(j+1)}) \Delta r_{(j)} \quad (21)$$

into $\Omega_{(j+1)}$ and then $\Omega_{(j+1)}$ into (19), we obtain a nonlinear equation in one unknown variable $g_{(j+1)}$. This equation can easily be solved by the Newton method.

To integrate Equations (11) – (14), the same implicit scheme is applied as for the spatial integration (the upper index stands for time):

$$T_r^{i+1} = T_r^i + \frac{1}{2} (\dot{T}_r^i + \dot{T}_r^{i+1}) \Delta t, \quad (22)$$

$$T_\theta^{i+1} = T_\theta^i + \frac{1}{2} (\dot{T}_\theta^i + \dot{T}_\theta^{i+1}) \Delta t, \quad (23)$$

$$T_z^{i+1} = T_z^i + \frac{1}{2}(\dot{T}_z^i + \dot{T}_z^{i+1})\Delta t, \quad (24)$$

$$e^{i+1} = e^i + \frac{1}{2}(\dot{e}^i + \dot{e}^{i+1})\Delta t. \quad (25)$$

Equations (22)–(25) are written for a given material point. The coordinates of the material points are updated by the integration of the velocity:

$$r^{i+1} = r^i + \frac{1}{2}(v^i + v^{i+1})\Delta t. \quad (26)$$

The time derivatives in (22)–(25) are functions of T_r , T_θ , T_z , g , v , r and e according to (11)–(14). The system (22)–(26) can be written as:

$$\mathcal{F}^{i+1} = \mathcal{F}^i + \frac{1}{2}\left\{\dot{\mathcal{F}}(\mathcal{F}^i, v^i, g^i) + \dot{\mathcal{F}}(\mathcal{F}^{i+1}, v^{i+1}, g^{i+1})\right\}\Delta t, \quad (27)$$

where \mathcal{F} denotes the column of the five quantities T_r , T_θ , T_z , e , r . Given \mathcal{F}^i , the system (27) can be solved for \mathcal{F}^{i+1} via successive approximations:

$$\mathcal{F}_{[n]}^{i+1} = \mathcal{F}^i + \frac{1}{2}\left\{\dot{\mathcal{F}}(\mathcal{F}^i, v^i, g^i) + \dot{\mathcal{F}}(\mathcal{F}_{[n]}^{i+1}, v_{[n]}^{i+1}, g_{[n]}^{i+1})\right\}\Delta t, \quad (28)$$

where the lower index in square brackets refers to the iteration number. Each iteration involves the integration of (17) as described above.

Equation (17) from which the velocity is found was obtained by the differentiation of the equilibrium equation (10) with respect to time. This actually means that, when solving the problem, the condition of equilibrium for the stresses is replaced with the condition of equilibrium for the stress rates. Analytically, if the initial stresses at $t = 0$ and the stress rates at $t \geq 0$ obey equilibrium, the stresses will also obey equilibrium at $t > 0$. However, during the numerical step-by-step time integration, if only the stress-rate equilibrium is controlled, the residual in the stress equilibrium may accumulate and thus lead to an increase in the error of the solution. In order to avoid this accumulation, at each time step, before solving (17), we calculate the stress residual, divide it by Δt to obtain the time derivative and substitute this quantity with the opposite sign into the right-hand side of (17).

5. Numerical solutions

An infinite body in the numerical calculations is modelled by taking $r_b^0 \gg r_a^0$. The accuracy of the approximation to an infinite body depends on the ratio r_b^0 / r_a^0 . Whether the outer radius is large enough can be judged from the change in the circumferential and axial components of the stress tensor at r_b (the radial stress is constant according to the boundary condition). The calculations showed that the minimum ratio r_b^0 / r_a^0 which ensures a less than 0.1% variation in the axial and circumferential stresses at r_b upon a twofold increase in the cavity radius varies from 200 for loose sand ($I_p^* \approx 0$) to 400 for dense sand ($I_p^* \approx 0.9$). The number of

the discretization points in the calculations is up to 300, with a higher degree of discretization in the vicinity of the cavity. One time step corresponds to a relative increment of 10^{-4} to 5×10^{-4} in the cavity radius.

Figure 1 shows the pressure components and the void ratio at the cavity wall as functions of the cavity radius during the expansion from $r_a^0 = 1$ to $r_a = 5$ calculated for Ticino sand with a hydrostatic initial pressure of 100 kPa. (We write p for pressure which is positive for compression.) Different curves correspond to different initial values of the relative density I_p^* . As the cavity expands, the pressure components increase in magnitude and monotonically approach their limit values. As seen from the curves, for the stresses and the density at the cavity wall to reach the limit values with sufficient accuracy, the cavity has to expand up to $r_a \approx 3 r_a^0$ for loose sand and up to $r_a \approx 4 r_a^0$ for dense sand.

The fact that the stresses and the void ratio at the cavity wall approach certain values and do not change any more with the deformation signifies that the state of the sand approaches a critical state. The stresses in a critical state are determined by the conditions (5). Close inspection of the constitutive function reveals that the conditions (5) define only the ratios between the stress components in a critical state, while the absolute values of the stresses remain arbitrary. From this it follows that the ratios between the limit values of the pressure components are constants for a given soil and do not depend on the initial density and pressure.

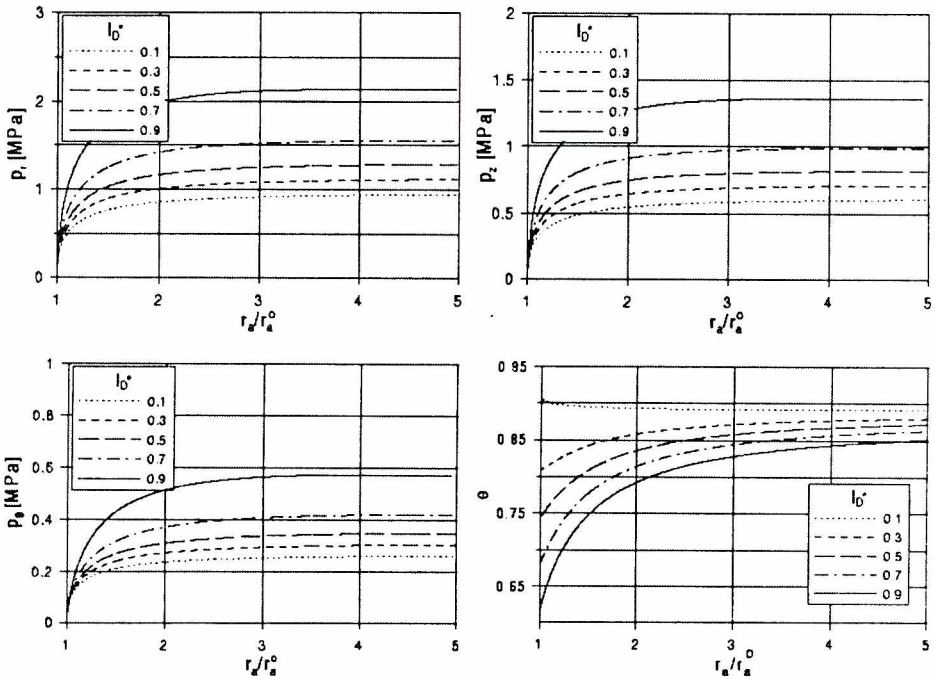


Figure 1. Expansion of a cylindrical cavity in Ticino sand. The pressure components and the void ratio at the cavity wall as functions of the cavity radius

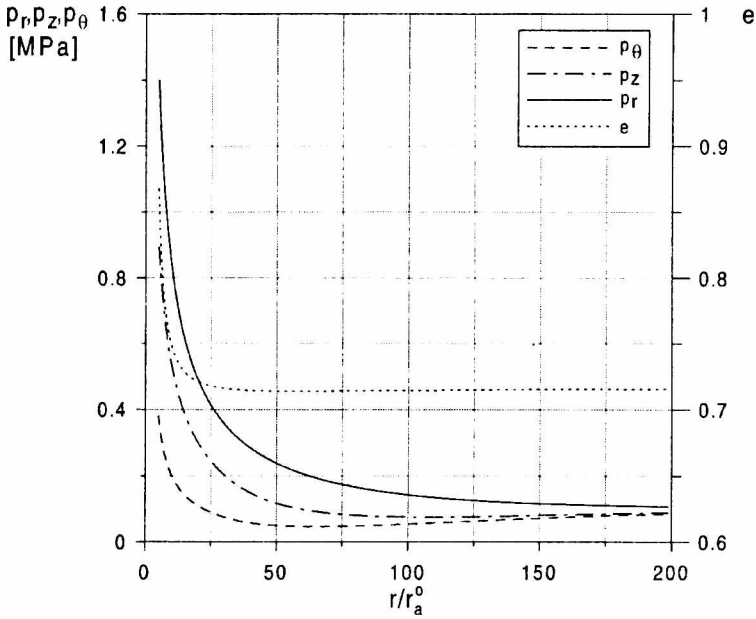


Figure 2. Spatial distribution of the pressure components and the void ratio after the expansion of a cavity. $I_b^* = 0.6$, $p_0 = 0.1$ MPa

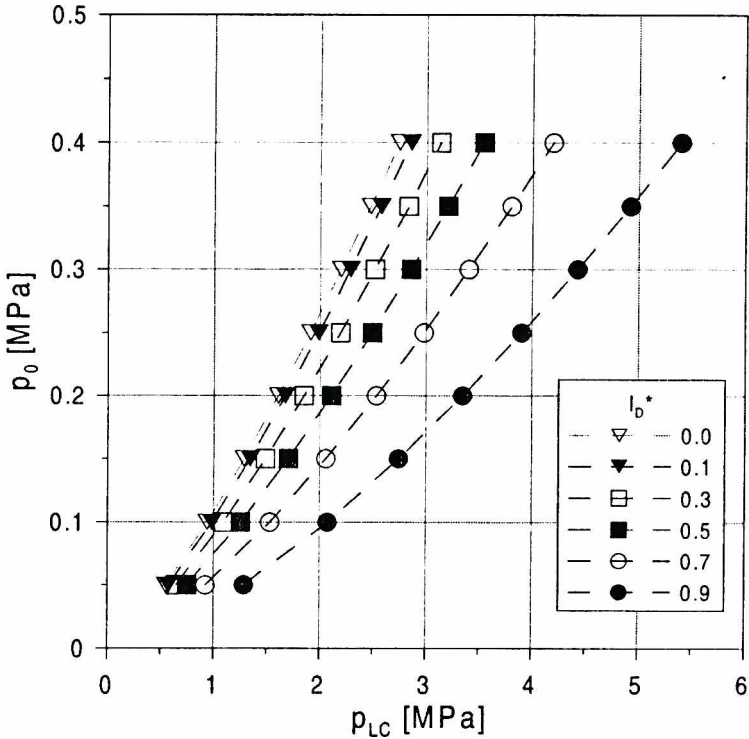


Figure 3. The limit pressure p_{LC} versus the initial pressure p_0 for different initial relative densities I_b^* . $K = 1.0$

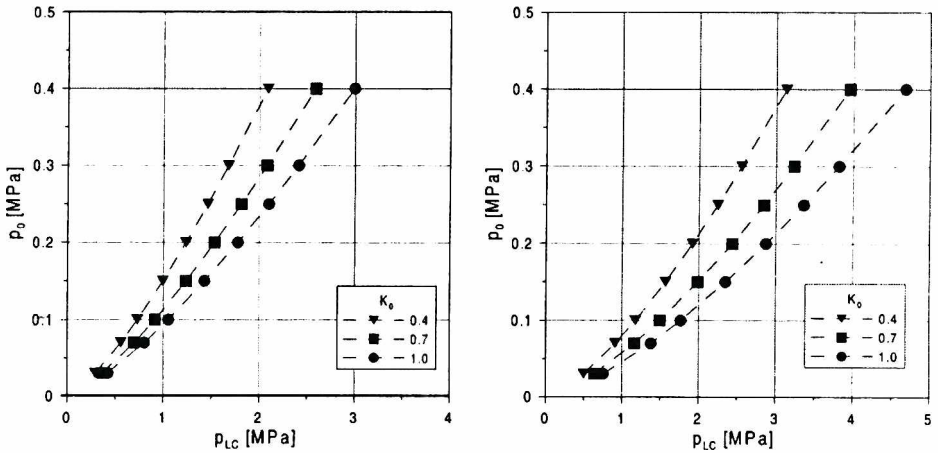


Figure 4. The limit pressure p_{LC} versus the initial pressure p_0 for different values of K_0 . $I_D^* = 0.2$ (on the left), $I_D^* = 0.8$ (on the right)

If a cavity expands in an infinite body and the initial state is homogeneous, each material element follows the same strain-stress path as an element at the cavity wall. As the cavity begins to expand, the pressures p_0 and p_z in each point first slightly decrease and the material contracts. This occurs at small strains when the change in the coordinate r of the point does not exceed a few per cent. This range cannot be seen at the scale of Figure 1. However, this is seen in Figure 2 which shows the spatial distribution of the pressure components and the void ratio after the expansion of the cavity from r_a^0 to $r_a = 5 r_a^0$.

The ratio of the limit radial pressure p_{LC} to the initial pressure p_0 depends on the initial density: the higher the density, the bigger the pressure change. Figure 3 shows the limit radial pressure p_{LC} as a function of the initial pressure p_0 and the initial relative density I_D^* . The influence of the coefficient $K = T_r^0/T_z^0$ on the limit pressure is shown in Figure 4. At the same initial mean pressure, the limit pressure is lower for a smaller K .

6. Comparison with experiments

The problem of expansion of a cylindrical cavity may serve as a model of the deformation of the soil during so-called pressuremeter tests. These tests are widely used in geotechnical practice for the evaluation of the state of soil in the field. Pressuremeter tests can also be conducted in the laboratory in large calibration chambers where the initial state of the soil is known. Experimental data of such tests available in the literature allow us to compare the results of the theoretical modelling with the corresponding values measured in the experiments.

The use of the symmetric cavity expansion problem considered above implies that we neglect possible loss of symmetry due to the shear band formation that may occur in the vicinity of the cavity, and assume that the length of the pressuremeter is large enough for the plane-strain conditions to be satisfied.

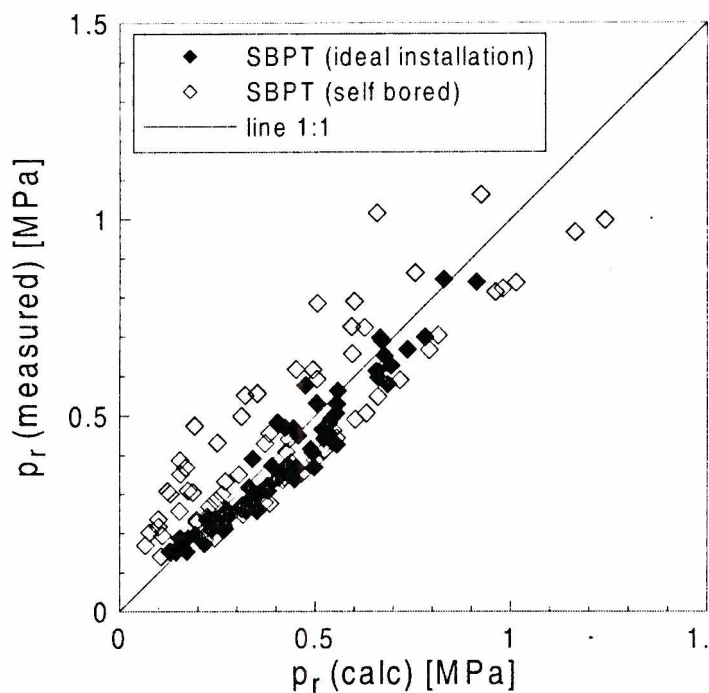


Figure 5. Comparison of the measured and the calculated radial pressures for $0.01 < \Delta r_a / r_a^0 < 0.1$

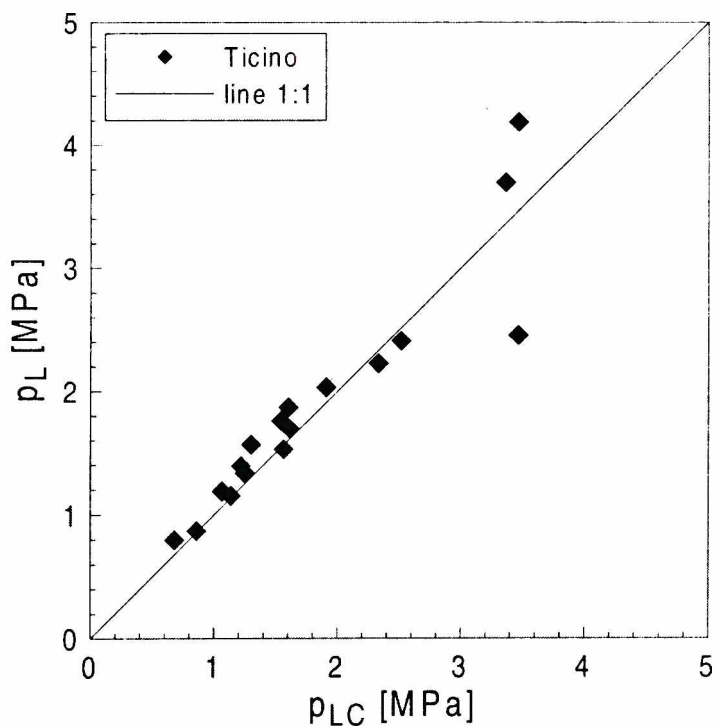


Figure 6. Comparison of the measured and the calculated limit pressures

There are two difficulties in comparing numerical solutions to the cavity expansion problem with experimental data on pressuremeter tests. First, the installation of a pressuremeter in the soil inevitably leads to the disturbance of the soil around the pressuremeter. As a consequence, the initial state of the soil becomes inhomogeneous and actually unknown. The disturbance of the soil is minimized on the “ideal” installation when a pressuremeter is put in an empty calibration chamber which is then filled with soil. The second difficulty in the interpretation of experimental results consists in the fact that the maximum achievable increase in the cavity radius in pressuremeter tests is usually too small to reach and measure the limit pressure. The maximum possible increase in the cavity radius depends on the type of pressuremeter; it ranges from 20 % for self-boring pressuremeters to 100 % for cone pressuremeters. Since the limit pressure cannot be measured directly, its determination requires special extrapolation methods (Baguelin *et al.* [13]), which leads to an uncertainty in the estimation.

Figures 5, 6 compare the numerical solutions to the cavity expansion problem considered above with the experimental data on pressuremeter tests conducted by Bellotti *et al.* [14] and Manassero [15] for Ticino sand in large calibration chambers with a self-boring pressuremeter. Figure 5 compares the calculated and the measured radial pressures at different stages at the beginning of the expansion in the range $0.01 < \Delta r_a / r_a^0 < 0.1$. The points in the figure encompass various initial stresses and densities. As expected, the scatter of the points about the bisectrix is wider for the usual installation than for the ideal installation. The limit pressures obtained from the experimental pressure-expansion curves by extrapolation (Manassero [15]) are compared in Figure 6 with the calculated values. Except for two points, the agreement is better than in Figure 5 and does not depend on the installation technique. This indicates that the disturbance introduced in the state of the soil during the installation of a self-boring pressuremeter has no considerable effect on the limit pressure.

7. Comparison with another model

In this section, for comparison purposes, we discuss the solutions to the cavity expansion problem obtained by Collins *et al.* [4] with the use of a critical-state elastic-plastic model based on the concept of state parameter (Been and Jefferies [16]). Like the hypoplasticity constitutive relation, that model describes the main features of the behaviour of granular materials under monotonic loading, including pressure and density dependent dilatancy, stiffness and critical states. The critical state line $e_c(p)$, where e_c is the critical void ratio and p is the mean pressure, is a straight line in the $(e, \ln p)$ -plane:

$$e_c = \Gamma - \lambda \ln(p/p_1) \quad (29)$$

with parameters Γ , λ and the reference pressure $p_1 = 1$ kPa. The behaviour of the material depends on both the mean pressure and the void ratio through the state parameter ξ defined as:

$$\xi = e - e_c, \quad (30)$$

where e_c is given by (29). The sign of the plastic volumetric strain in shear is determined by the sign of ξ so that the state of the material tends to a critical state. The difference between the angles of internal friction in a given state, φ , and in a critical state, φ_c , is assumed to be in the form (Been and Jefferies [16]):

$$\varphi - \varphi_c = A[\exp(-\xi) - 1], \quad (31)$$

where A is a parameter in the range 0.6–0.95, and the angles are measured in radians. The flow rule is defined by the dilation angle ψ taken to be equal to $(5/4)(\varphi - \varphi_c)$. The shear modulus in the elastic zone is assumed to vary with the mean pressure and the void ratio according to an empirical relation proposed by Richart *et al.* [17].

Collins *et al.* [4] considered the expansion of a cavity from zero radius with $K = T_v^0/T_z^0 = 1$ and obtained a self-similar solution. In this case the pressure at the cavity wall may be viewed as the limit pressure for a cavity which expands from a finite radius. The limit pressure p_{LC} calculated for a cylindrical cavity as a function of the initial values of the void ratio e_0 and the mean pressure p_0 is approximated by the formula:

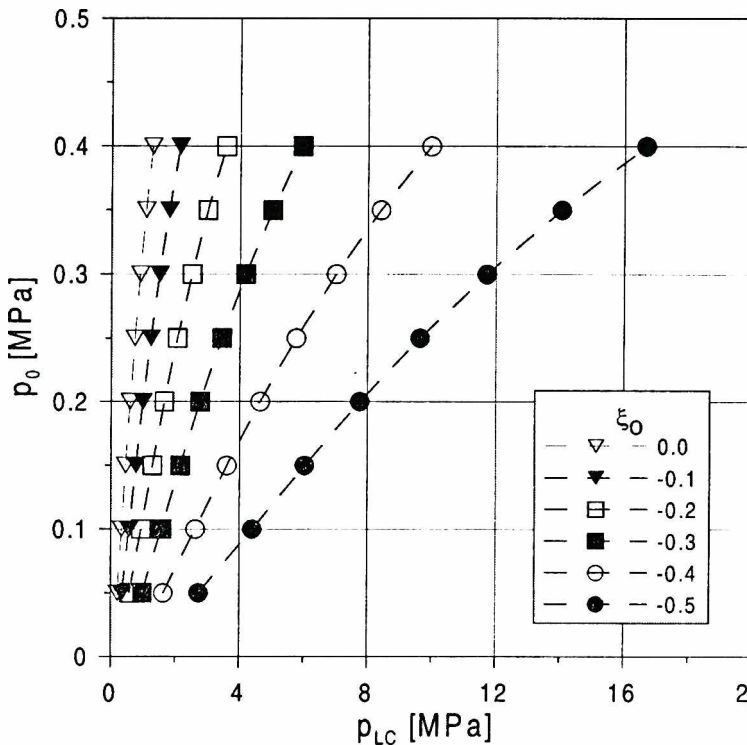


Figure 7. The limit pressure p_{LC} for a cylindrical cavity versus the initial pressure p_0 for different initial state parameters ξ_0 calculated for Ticino sand by Collins *et al.* [4]

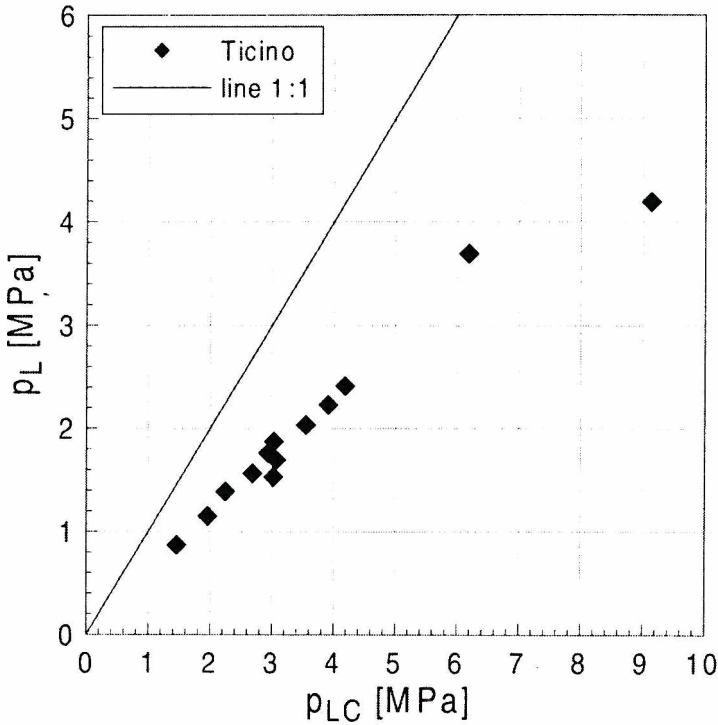


Figure 8. The limit pressure p_{LC} calculated by Collins et al. [4] versus the experimental values p_L from PMT

$$\frac{p_{LC}}{p_0} = c_1 p_0^{c_2 + c_3 v_0} \exp(-c_4 v_0), \quad (32)$$

where $v_0 = 1 + e_0$, p_0 is in kPa, and the constants c_1, \dots, c_4 for Ticino sand in the range $25 \text{ kPa} < p_0 < 1000 \text{ kPa}$, $-0.5 < \xi_0 < 0.1$ are the following: $c_1 = 5.453 \times 10^5$, $c_2 = -0.702$, $c_3 = 0.268$, $c_4 = 5.142$.

Figure 7 shows the limit pressure p_{LC} calculated with (32) as a function of the initial mean pressure p_0 and the state parameter ξ_0 . As in the hypoplastic model, see Figure 3, the limit pressure increases with increasing initial density and pressure. Figure 8 shows the limit pressure (32) predicted by the elastic-plastic model in comparison with the experimental values (the experimental data are the same as in Figure 6, with $K \approx 1$). The calculated limit pressures are higher than the measured ones by a factor of 1.6 to 2.0. Assuming that the solution reproduced here is correct, the discrepancy is to be attributed to the constitutive model. The main reason for the error is that the constitutive theory and, specifically, relation (31) used for the calculations are based on triaxial compression tests with constant radial pressure. The stress-strain path of a material element during the expansion of a cavity, either spherical or cylindrical, differs from that in a triaxial compression test with constant radial pressure. Since the behaviour of granular materials is strongly path-dependent, the use of (31) may result in a large error. Other sources of the error may be the compression law (29) which holds true only for pressures below 1 MPa

(Been *et al.* [18], Konrad [19], Ishihara [20]), and the empirical formula of Richart *et al.* [17] used for the evaluation of the state-dependent elastic shear modulus.

8. Conclusion

The problem of the symmetric quasi-static large-strain expansion of a cylindrical cavity in sand is solved with the constitutive equation of hypoplasticity. As the cavity expands, the stresses and the density at the cavity wall asymptotically approach limit values which correspond to a critical state of the sand. For given sand, the limit values depend on the initial stresses and the initial density. The limit pressures calculated for Ticino sand are in good agreement with the experimental results of pressuremeter tests for the same sand. The dependence of the limit pressure on the initial state makes it possible to use the cavity expansion problem in geotechnical applications for the evaluation of the state of soil in the field from the results of pressuremeter tests [24].

Appendix

Here we write the formulae for the coefficients in the constitutive function (2). For a detailed discussion see [6–8].

The factor a is determined by the friction angle φ_c in critical states:

$$a = \sqrt{\frac{3}{8}} \frac{(3 - \sin \varphi_c)}{\sin \varphi_c}. \quad (33)$$

The factor F is a function of $\hat{\mathbf{T}}^*$:

$$F = \sqrt{\frac{1}{8} \tan^2 \psi + \frac{2 - \tan^2 \psi}{2 + \sqrt{2} \tan \psi \cos 3\theta}} - \frac{1}{2\sqrt{2}} \tan \psi, \quad (34)$$

where

$$\tan \psi = \sqrt{3} \|\hat{\mathbf{T}}^*\|, \quad \cos 3\theta = -\sqrt{6} \frac{\text{tr}(\hat{\mathbf{T}}^{*3})}{[\text{tr}(\hat{\mathbf{T}}^{*2})]^{3/2}}. \quad (35)$$

Three characteristic void ratios are specified as functions of the mean pressure: the void ratio of maximal densification, e_d , the critical void ratio, e_c , and the void ratio in the loosest state, e_l . The pressure dependence of these void ratios is postulated in the form:

$$\frac{e_i}{e_{i0}} = \frac{e_c}{e_{c0}} = \frac{e_d}{e_{d0}} = \exp \left[- \left(\frac{-\text{tr} \mathbf{T}}{h_s} \right)^n \right], \quad (36)$$

with the corresponding reference values e_{i0} , e_{c0} , e_{d0} for zero pressure ($e_{i0} > e_{c0} > e_{d0}$). The constants e_{i0} , e_{c0} , e_{d0} together with h_s , n are material parameters. The factors

$$f_c = \left(\frac{e_c}{e} \right)^\beta, \quad f_d = \left(\frac{e - e_d}{e_c - e_d} \right)^\alpha \quad (37)$$

are called the pycnotropy functions, and the factor:

$$f_b = \frac{h_s}{n} \left(\frac{1 + e_i}{e_i} \right) \left(\frac{e_{i0}}{e_{c0}} \right)^\beta \left(\frac{-\text{tr} \mathbf{T}}{h_s} \right)^{1-n} \left[3 + a^2 - \sqrt{3} a \left(\frac{e_{i0} - e_{d0}}{e_{c0} - e_{d0}} \right)^\alpha \right]^{-1} \quad (38)$$

is called the barotropy function, where α and β are material parameters.

The calibration procedure for the determination of the constitutive parameters is described by Herle and Gudchus [9] and Herle [21]. For purposes of the present study the constitutive function (2) was calibrated for Ticino sand with the use of the experimental data of Been [22] and Giuliano [23]. The constitutive parameters of Ticino sand are given in the table below.

h_s [MPa]	n	e_{c0}	e_{d0}	e_{r0}	φ [°]	α	β
250	0.68	0.94	0.59	1.11	31	0.11	1.0

References

- [1] Vesić A. S., *Expansion of cavities in infinite soil mass*, J. Soil Mech. Found. Div., Proc. ASCE **98**, 265, 1972
- [2] Carter J. P., Booker J. R. and Yeung S. K., *Cavity expansion in cohesive frictional soils*, Géotechnique **36**, 349, 1986
- [3] Yu H. S. and Houlsby G. T., *Finite cavity expansion in dilatant soils: loading analysis*, Géotechnique **41**, 173, 1991
- [4] Collins I., Pender M. and Yan W., *Cavity expansion in sands under drained loading conditions*, Int. J. Num. Anal. Meth. Geomech. **16**, 3, 1992
- [5] Shuttle D. and Jefferies M., *Dimensionless and unbiased CPT interpretation in sand*, Int. J. Num. Anal. Meth. Geomech. **22**, 351, 1998
- [6] Gudchus G., *A comprehensive constitutive equation for granular materials*, Soils and Foundations **36**, 1, 1996
- [7] Bauer E., *Calibration of a comprehensive hypoplastic model for granular materials*, Soils and Foundations **36**, 13, 1996
- [8] von Wolffersdorff P. A., *A hypoplastic relation for granular materials with a predefined limit state surface*, Mechanics of cohesive-frictional materials **1**, 251, 1996
- [9] Herle I. and Gudchus G., *Determination of parameters of a hypoplastic constitutive model from properties of grain assemblies*, Mechanics of Cohesive-frictional Materials **4**, 461, 1999
- [10] Schofield A. N. and Wroth C. P., *Critical State Soil Mechanics*, McGraw-Hill, London, 1968
- [11] Been K., Jefferies M. G. and Hachey J., *The critical state of sands*, Géotechnique **41**, 365, 1991

-
- [12] Poulos S. J., *The steady state of deformation*, J. Geotech. Eng. Div., Proc. ASCE **107**, GT5, 553, 1981
- [13] Baguelin F., Jézéquel J. F. and Shields D. H., *The Pressuremeter and Foundation Engineering*, Trans. Tech. Publication, Clausthall, 1978
- [14] Bellotti R., Ghionna V., Jamiolkowski M., Robertson P. K. and Peterson R. W., *Interpretation of moduli from self-boring pressuremeter tests in sand*, Géotechnique **39**, 269, 1989
- [15] Manassero M., *Calibration chamber correlations for horizontal in situ stress assessment using self-boring pressuremeter and cone penetration tests*, In A. B. Huang (editor), Calibration chamber testing, Elsevier, 237, 1991
- [16] Been K., Jefferies M., *A state parameter for sands*, Géotechnique **35**, 99, 1985
- [17] Richart F. E., Hall J. R. and Woods R. D., *Vibrations of soils and foundations*, Prentice-Hall, Englewood Cliffs, 1970
- [18] Been K., Jefferies M. G. and Hachey J., *The critical state of sands*, Géotechnique **41**, 365, 1991
- [19] Konrad J. M., *In situ sand state from CPT: evaluation of a unified approach at two CANLEX sites*, Can. Geotech. Journal **34**, 120, 1997
- [20] Ishihara K., *Liquefaction and flow failure during earthquakes*, Géotechnique **43**, 351, 1993
- [21] Herle I., *Hypoplastizität und Granulometrie einfacher Korngerüste*, Veröffentlichungen des Institutes für Bodenmechanik und Felsmechanik der Universität Karlsruhe, **142**, 1997
- [22] Been K., private communication, 1996
- [23] Giuliano G., *Analisi della comprimibilità delle sabbie del ticino e di Hokksund da prove triassiali. Tesi di Laurea*, Dipartimento di Ingegneria Strutturale, Facoltà di Ingegneria, Politecnico di Torino, Torino, 1987
- [24] Cudmani R. and Osinov V. A., *The cavity expansion problem for the interpretation of cone penetration and pressuremeter tests* (submitted)